

Evaluation of the Effects of using Central Pattern Generators to Synchronize the Undulating Motion of a Bio-Inspired Robotic Fin Testbed

Albert A. Espinoza, MSME^{id}, Paola C. Alvarez Echevarria, BSME^{id}

Universidad Ana G. Méndez – Gurabo, PR, USA, espinozaa1@uagm.edu, palvarez20@email.uagm.com

Abstract– *Unmanned Underwater Vehicles (UUVs) with bio-inspired fin propulsion systems have captivated the interest of many researchers in recent years, particularly because such systems provide higher dexterity and energy efficiency, and less environment perturbation when compared to conventional propeller-based propulsion. Bio-inspired propulsion UUVs designs are typically based on large chains of articulated actuators, which must be properly synchronized to achieve the desired UUV gait motion. To achieve this task, a control strategy based on artificial Central Pattern Generators (CPGs) is commonly used. CPGs provide a highly stable, smooth, synchronized controlled transition of a large number of individually driven actuators, but solving the dynamic equations of the CPG model results in an increase in the computing requirements of the UUV microcontroller, which may limit its implementation on UUVs with a high number of actuators and microcontroller with limited computing power. Thus, the purpose of this work is to evaluate the feasibility and limitations of implementing a CPG-based locomotion control strategy on an Arduino® Mega platform to drive a 16-actuator articulated testbed of an undulating robotic fin, as well as the dynamic effects of the CPG control strategy. The results demonstrate that a CPG can be implemented on the Arduino® Mega platform by optimizing the structure of the CPG equations while still maintaining the favorable qualities of CPG-based control when compared to a direct undulating wave-based control approach.*

Keywords—*Unmanned Underwater Vehicles (UUVs), Central Pattern Generators (CPGs), Undulating Fin Propulsion, Bio-inspired UUVs, Control*

I. INTRODUCTION

Bio-inspired underwater propulsion systems have gained increased attention in the development of unmanned underwater vehicle (UUV) robotic systems in recent years, mainly because they provide a more natural, dexterous, and energy efficient means of achieving underwater motion without causing excessive turbulence compared to conventional propeller-type propulsion [1]. For instance, the black ghost knifefish (See Figure 1) is capable of maneuvering in tight spaces, station-keeping, swimming forward and backward, and achieving high swimming speeds with the help of its undulating dorsal fin [2]. The ghost knife achieves this high dexterity by actively modulating the frequency, amplitude, and traveling direction of the undulating fin wave motion [3]. These features make bio-inspired propulsion methods particularly useful in underwater surveying, underwater life monitoring, sea floor

exploration, among other underwater applications that require navigation in remote, hard to reach places without excessive perturbation to marine life ecosystems.



Figure 1. Photo of *Apteronotus albifrons* - black ghost knifefish (Photo credit: Per Erik Sviland)

UUVs with bio-inspired propulsion systems usually consist of several articulated actuators that either replicate the flexibility of fish anatomy with rigid fins [4-9] or mimic the undulating motion of the fin itself [10-14]. Controlling and synchronizing the motion of chains of actuators requires a sophisticated control methodology, particularly in UUVs that undergo sudden transitions between different swimming gaits. To properly synchronize actuator motion, fin-based propulsion UUVs controllers rely on the use of artificial Central Pattern Generators (CPGs). Artificial CPGs are bio-inspired mathematical dynamic models that are used to produce synchronized, rhythmic motion gaits or patterns for articulated robots which are based on a series of many dynamically coupled actuators, while allowing for a smooth transition when significant changes are made to the parameters of the undulating wave [13]. Some examples of CPG-based locomotion used in UUVs with articulated undulating fins can be found in [10-14]. While CPGs simplify the structure of the low-level control of the fin actuators, one of the potential drawbacks of using CPGs is the increased computation cost required to compute the CPG dynamics, which may limit its implementation on UUVs with a high number of actuators and microcontroller with limited computing power.

The purpose of this work is to evaluate the feasibility and limitations of implementing a CPG-based locomotion control strategy on an Arduino® Mega platform to drive a 16-actuator articulated testbed of an undulating robotic fin. Additionally,

Digital Object Identifier: (only for full papers, inserted by LACCEI).

ISSN, ISBN: (to be inserted by LACCEI).

DO NOT REMOVE

the dynamic effects of the CPG control strategy will be empirically evaluated and compared to a direct undulating wave-based control approach.

The rest of this paper is organized as follows. In Section II the mechanics of the undulating traveling wave kinematics and the dynamic model of the Central Pattern Generator will be presented. Section III describes the experimental testbed of the robotic fin used to evaluate the effects of CPG-based control. In Section IV, the results from the experiments are presented and discussed. Finally, Section V provides concluding remarks, as well as possible future work.

II. UNDULATING WAVE MECHANICS AND CENTRAL PATTERN GENERATOR DYNAMICS

The mechanics of a typical robotic undulating fin are presented in Figure 2. The mechanism is composed of N rigid fin rays mounted onto individual actuators with their axes of rotation aligned (in the x axis). Thus, the angular position of the i^{th} ray is defined by the angle, θ_i , about the x axis and referenced with respect to the positive z -axis (see Figure 2). The fin rays are mounted equidistantly along the x direction to simulate the dorsal fin of the Black Ghostfish (see Figure 1).

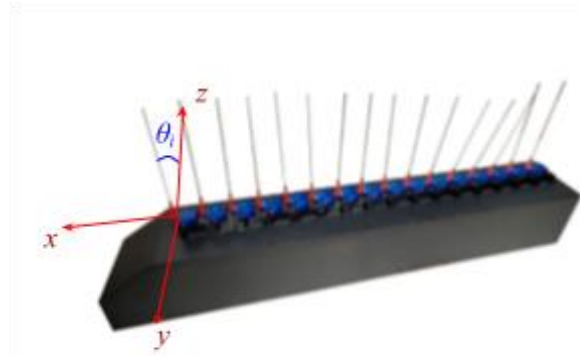


Figure 2. Robotic Undulating Fin Schematic

To create a traveling undulating wave, each fin ray must be prescribed a sinusoidal motion as defined by:

$$\theta_i(t) = A_i \sin(2\pi f_i t + \phi_i), \quad i = 1, \dots, 16 \quad (1)$$

Where A_i , f_i , and ϕ_i , represent the wave amplitude, frequency, and phase offset, respectively. Each of these three parameters can be independently controlled to achieve a desired UUV velocity and motion. For fixed, equally spaced, and serially aligned actuators along the fin, the phase offset is constant for all rays and is fully defined by the desired number of waves (oscillations) along the fin, ω , and the number of actuators/rays, N , according to the following:

$$\phi_i = \frac{2\pi\omega}{N-1}, \quad i=1, \dots, 16 \quad (2)$$

For the experimental setup used in this study, a total of 16 actuators were used to form one single period of the traveling wave (i.e., $\omega = 1$).

The implementation of the artificial CPG model is based on N coupled linearized dynamic oscillators [14], defined by the following:

$$\ddot{r}_i = \beta^2 (R_i - r_i) - 2\beta \dot{r}_i \quad (3)$$

$$\dot{\phi}_i = 2\pi f_i + \sum \omega_{ij} r_j \sin(\phi_j - \phi_i - \varphi_{ij}) \quad (4)$$

In the dynamic model above, r_i and ϕ_i define the dynamic state of the wave amplitude and phase offset of the i^{th} ray, respectively. The parameters ω_{ij} and φ_{ij} are defined as the coupling weights and phase shift bias from ray i to j , respectively. The selection of the specific values for the φ parameters is predetermined by the interconnection structure of the robotic fin design. For example, for rays 1 and 2, the desired phase shift bias weight is computed from Equation (2) and is taken as a lead angle (positive value) from ray 1 to ray 2 and as a lag angle (negative angle) from ray 2 to ray 1. The ω weights represent the strength of the interconnection between ray i and its neighboring rays. These weights are considered adjustable parameters that affect the rate of response of the CPG equations. β stands for the response gain parameter, which can be adjusted to modify the speed of response of the CPG dynamics. Finally, R_i and f_i are the i^{th} individual amplitude and frequency commands for ray i , respectively. These are the values that the CPG will settle to at steady state, as defined by Equations (3) and (4).

From the evolution of the CPG dynamics, the angular position of each i^{th} ray is given by:

$$\theta_i = r_i \cos \phi_i \quad (5)$$

Once implemented, the CPG can be thought of as a black box dynamic model that gradually transitions each individual ray angular position towards a final steady-state desired amplitude, frequency, and/or phase shift command. Figure 3 demonstrates a simulated angular position output from the CPG as a result to a sudden (i.e., step) change in amplitude command from 10° to 30° , while the frequency and phase shift commands are kept constant at values of π rad/s and 24° , respectively. Note that only the angular positions of the odd-numbered index rays (8 rays in total) are presented for clarity.

Figure 3 shows the gradual time evolution of the CPG dynamics. For the first step change in amplitude command from 0° to 10° , the angular position of each ray takes approximately 5 seconds to fully develop and settle to its final amplitude, frequency, and phase shift. For the second step change in amplitude command (10° to 30°) the CPG takes only about 1 second to reach the final values mainly because the frequency and phase shift were already at or close to their final values and

the only parameter that had to increase with time was the amplitude.

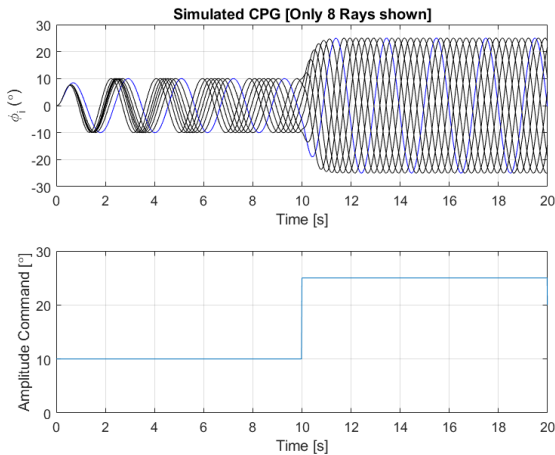


Figure 3. Simulated Central Pattern Generator (Only 8 rays shown)

III. EXPERIMENTAL SETUP

To evaluate the feasibility of implementing the CPG model on an Arduino® Mega platform, a testbed of a robotic fin was constructed consisting of 16 individual SG90 low-cost servomotors mounted such that their axes of rotation lie along the articulated fin longitudinal axis (See Figure 4). A small 3-D printed arm was then mounted to each servo to mimic the rays of the robotic fin. Large white circular markers were placed on top of each arm tip to allow for easier circular object detection of each ray tip, as seen from a video camera mounted directly above the robotic fin. Because the Arduino® Mega does not have 16 individual PWM ports to drive each servo, an Adafruit PCA9685 16-channel I²C servo driver was used.



Figure 4. Bio-inspired robotic fin testbed

To evaluate the performance of each fin ray control methodology used in this study, the angular position of each ray

was measured using a video camera along with object detection software based on MATLAB. A cell phone video camera was mounted directly above the robotic fin prototype keeping all 16 rays in its field of view. The camera can take 1920 x 1080-pixel images at 30 frames per second. The video feed was then processed one frame at a time by first converting the RGB color frame images to grayscale and then passed to a circle detection function in MATLAB (See Figure 5). The centroid location (in X and Y pixels) and the approximated radius (in pixels) for each detected circle was then stored to be extracted then processed offline by converting the pixel data to angular position and finally plotting the angular position trajectory of each fin ray. Figure 6 demonstrates a sample frame taken from the video-based angular position measurement process. The detected circle locations are shown by the red circles.

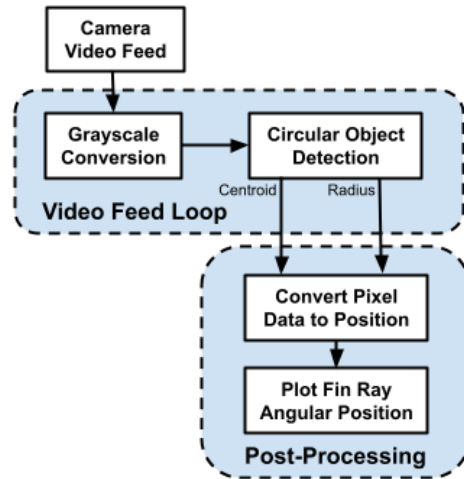


Figure 5. Video-based angular position measurement process

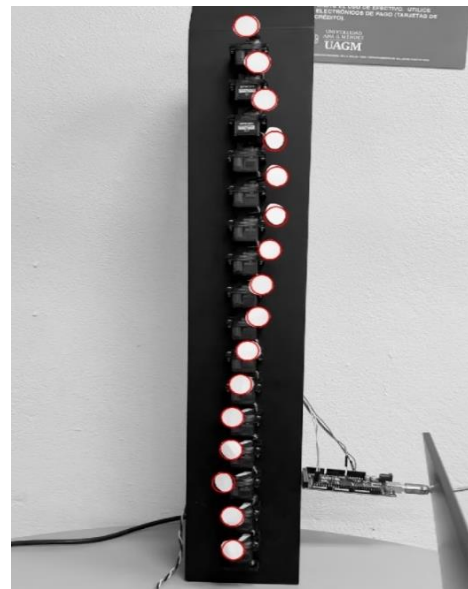


Figure 6. Sample circle object detection frame

The robotic fin prototype was tested under two different control scenarios. First, the fin ray angular position was controlled using a direct undulating wave-based control approach, in which each ray position is computed from Eq. (1). Secondly, the CPG model was implemented using Eqs. (2)-(5). For each control strategy, the effects of abruptly changing the desired amplitude and frequency undulating wave commands were independently tested. The angular position of each ray was recorded for comparison.

IV. TESTING RESULTS

The CPG model presented in Section II was successfully implemented in the Arduino® Mega board after optimizing the structure of the CPG dynamic equations in Eqs. (3) and (4) by taking advantage of the sparse structure of the coupling weights and phase shift bias matrices in Eq. (4). The numerical integrations were computed using the Euler integration method with a fixed time step of 0.02 s. The time step was selected to allow the Arduino to be able to complete each loop step within this time in a deterministic manner.

To compare the control strategies under abrupt changes to the wave frequency and amplitude commands, each strategy was individually implemented onto the Arduino® Mega board, video was recorded and then post-processed offline to gather angular position for each one of the 16 fin rays. Figure 7 shows sample angular position results for Ray 11 after applying abrupt changes to the wave frequency from 2π , π , and $\pi/2$ rad/s, keeping the amplitude and phase offset constant at 30° and 24° , respectively.

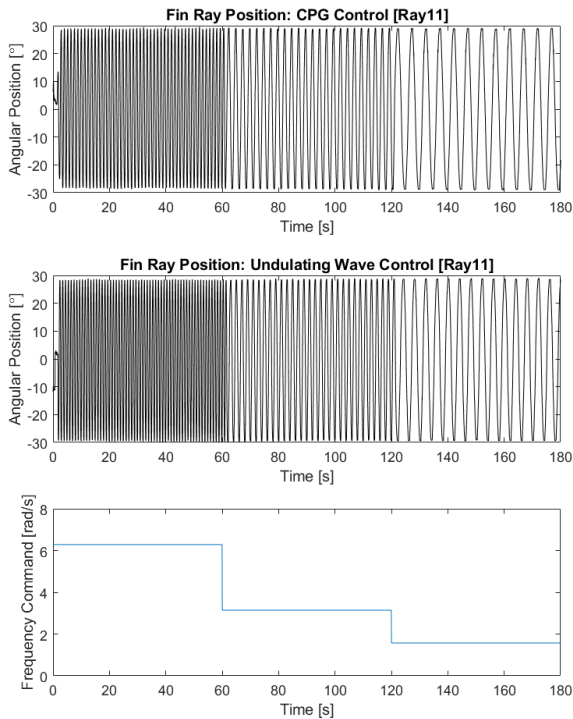


Figure 7. Sample angular position results under abrupt frequency changes.

The results appear to be similar in that the fin rays correctly ultimately change to the desired wave frequency. However, under closer inspection, as shown in the comparison graphs of Figure 8, the way in which the changes occur is slightly, yet importantly, different. Figure 8(b) and (c) shows that the direct wave motion control strategy, as expected, introduces a steep slope at around $t = 61$ and $t = 121$ seconds, which is due to the sudden change to the wave frequency occurring at exactly the 61 second and 121 second mark. In contrast, the CPG control strategy provides a more gradual, seamless transition from the previous frequency command to the next value at those same times that is difficult to identify with certainty the specific point in time in which the frequency change was commanded. It is worth mentioning that all other servos behaved in a similar way. The difference in response was also noticeable in the distinct sound made by the servo actuators as the system undergo each frequency change. The wave motion control strategy led to a louder, grinding noise coming from the gearbox of the servomotors, which demonstrates that the change in command occurs very suddenly and ultimately may be detrimental to the useful life of the servos.

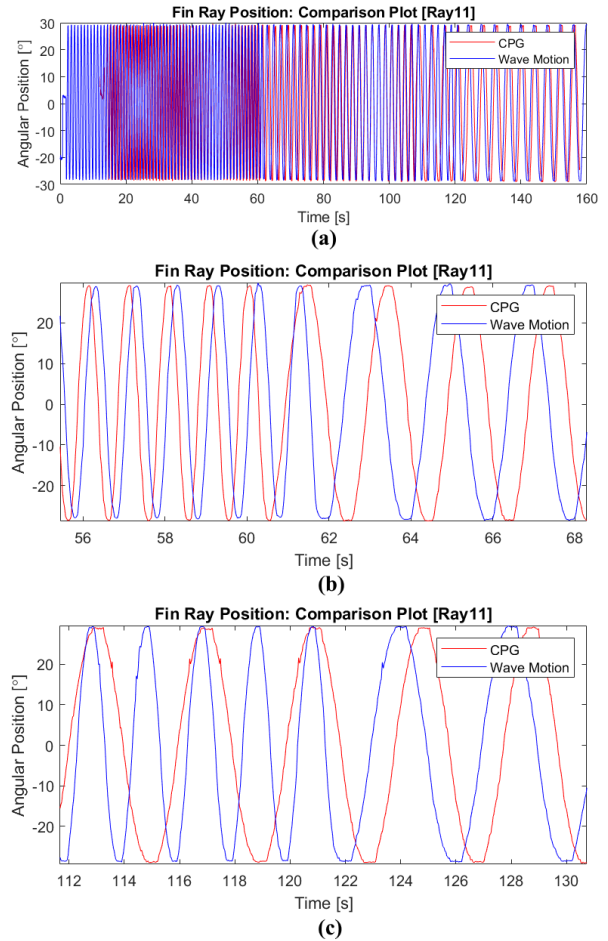


Figure 8. Comparison graphs for frequency changes: (a) complete graph, (b) zoom in on first change, (c) zoom in on second change

To compare the control strategies under abrupt changes to wave amplitude, the amplitude command was changed from 30° to 10° , then back to 30° , while keeping the frequency and phase offset fixed to 2π and 24° , respectively. Figure 9 shows sample results for Ray 10. It is worth noting that all others rays followed similar results. In this case, the transition differences are more evident. As evidenced by Figure 9, and with more detail in Figure 10, the transitions in the CPG control strategy are marked by a near-exponential amplitude transition, whereas the direct wave control is marked by sudden amplitude changes.

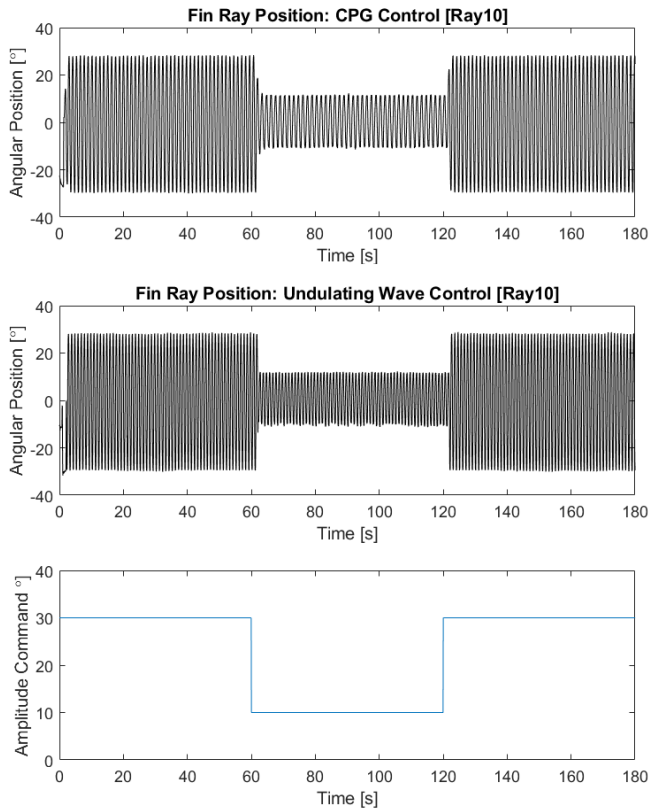


Figure 9. Sample angular position results under amplitude changes

Figure 10(b) shows a noticeable sudden dip in the angular position in the direct wave motion control curve at $t = 62$ seconds, which shows that the transition changes suddenly regardless of when in time the command change is applied. This can be highly problematic in the control of the entire fin because the inter-ray angular position difference between neighbouring actuators has significant constraints imposed on it by the flexible mesh material used to create the fin itself. This inter-ray angular difference cannot be too large or else the mesh material can tear or get stretched beyond its elastic limits. This issue is not observed in the CPG control approach because all rays will transition exponentially from their position before the amplitude command change to their new final angular position after the amplitude command change. Furthermore, there was

also a noticeable difference in the sound coming from the actuators at the transition time. The direct wave control strategy caused a loud grinding noise in the gearbox of the servomotors, whereas the CPG strategy had a much lower sound occur near the transition times. This is due to the fact that each servo is commanded to change position immediately without regards to where the servo is currently located. This may cause significant damage to the servos and a noticeable reduction in useful life.

One potential drawback of the CPG approach may be the overall settling time the transition may take to reach its final steady-state in all parameters (i.e., frequency, amplitude, phase offset). Figure 10(b) shows that although the amplitude transitions rather quickly (less than 2 seconds), the frequency and phase offset take a bit longer to reach final steady values (approximately 8 seconds in total).

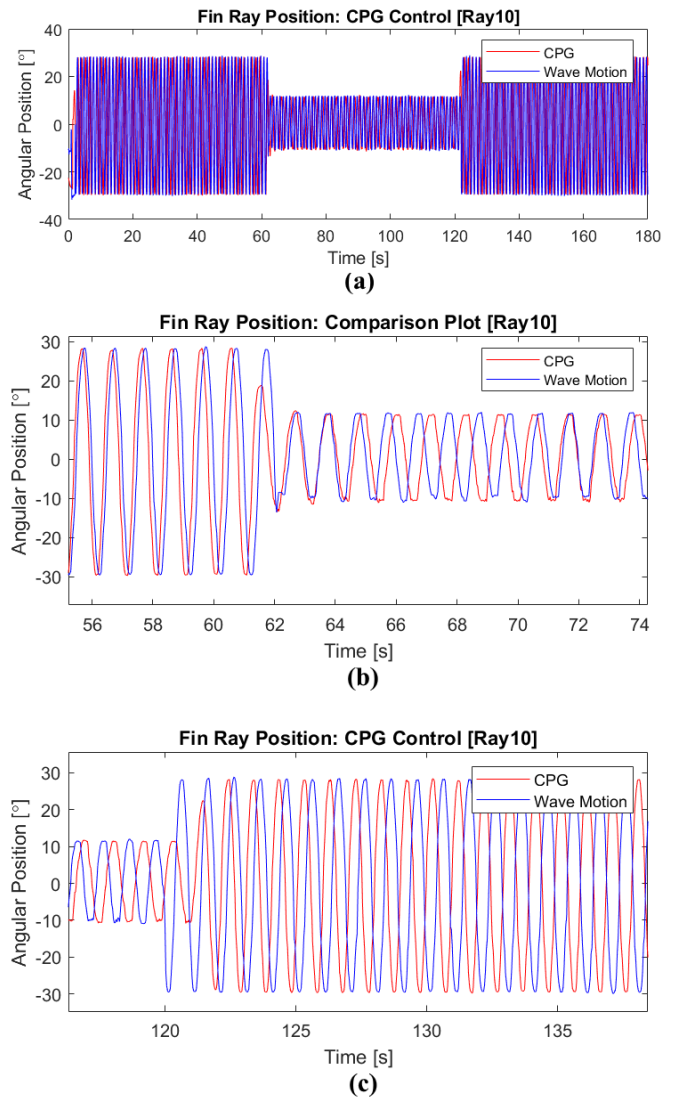


Figure 10. Comparison graphs for amplitude changes: (a) complete graph, (b) zoom in on first change, (c) zoom in on second change

The relatively slow response may be problematic in applications in which fast control commands are required, such as those needed for agile manoeuvring or obstacle avoidance under fast swimming. However, it is worth mentioning that the transition dynamics can be further optimized to specific controller response requirements by actively adjusting the coupling weights and the response gain parameter, the β and ω_{ij} parameters in Eqs. (3) and (4). This adjustable dynamic response is another added benefit of the CPG control approach, which is not possible under the direct wave motion control approach.

V. CONCLUSION

The results obtained in this study demonstrate that a control strategy based on an artificial central pattern generator (CPG) dynamic model can be successfully implemented in a system with limited computing power, such as an Arduino® Mega board, by optimizing the code and reducing the number of loop iterations by exploiting the sparse matrix structure of the CPG equations under the specific case of spatially equidistant, fixed, sequentially positioned actuators with a common axis of rotation. For this study, the CPG dynamics were successfully solved using a Euler integration approach with a fixed time step of 0.02 seconds, which was found to be enough time to accommodate both the computation of the CPG equations as well as the amount of time required to send the motion commands to all 16 actuators over serial communication.

The CPG control approach was successfully compared to a direct undulating wave control approach under abrupt changes in wave frequency and amplitude commands. The results demonstrate that under both frequency and amplitude abrupt change scenarios, the CPG control approach provides significant benefits in terms of smoother, stable transitions and a coordinated motion of all the actuators of the articulated robotic fin testbed. This feature may significantly help improve the life of the servomotors and prevent structural failures in the materials used to construct the robotic fin mesh. The only particular drawback of the CPG approach is the inherent settling delay in the transition dynamics. However, by selecting suitable optimized dynamic parameters, the CPG control approach can be used to simultaneously control a high number of actuators using computing systems with limited computing power. A study of the effects and optimization strategies of these dynamic parameters for the use of CPGs in UUVs with undulating fin propulsion systems is a possible avenue for future work. Furthermore, the CPG control strategy will also be implemented on a robotic fin prototype testbed that will be submerged in water and free to move along the longitudinal axis of the fin to assess the swimming performance of this CPG control strategy under more realistic underwater operating conditions.

ACKNOWLEDGMENT

The authors would like to gratefully acknowledge the financial support provided to this project by the Puerto Rico Louis Stokes Alliance for Minority Participation (PR-LSAMP), NSF Award Number: HRD-2008186, the Consortium of Hybrid Resilient Energy Systems (CHRES), sponsored by the U.S. Department of Energy (DOE), Award Number DE-NA0003982, the Puerto Rico Energy Center (PREC), and the Mechanical Engineering Department of the José Domingo Pérez School of Engineering at Universidad Ana G. Méndez, Gurabo Campus.

REFERENCES

- [1] I. Neveln, et al., "Biomimetic and bio-inspired robotics in electric fish research," *The Journal of Experimental Biology*, 216 (Pt 13): 2501-14, 2013.
- [2] P. Webb, "Maneuverability - general issues," *IEEE J. Ocean. Eng.* 29(3), 547-555 (2004).
- [3] O. Curet, N. Patankar, G. Lauder, and M. A. MacIver, "Mechanical properties of a bio-inspired robotic knifefish with an undulatory propulsor," *Bioinspiration Biomimetics* 6(2), 026004 (2011).
- [4] Wang W, Xie G. "CPG-based Locomotion Controller Design for a Boxfish-like Robot," *International Journal of Advanced Robotic Systems*. 2014;11(6). doi:10.5772/58564.
- [5] A. Crespi, D. Lachat, A. Pasquier, et al., "Controlling swimming and crawling in a fish robot using a central pattern generator," *Autonomous Robots* 25, 3-13 (2008). <https://doi.org/10.1007/s10514-007-9071-6>.
- [6] C. Wang, et al. "CPG-Based Locomotion Control of a Robotic Fish: Using Linear Oscillators and Reducing Control Parameters via PSO," *International Journal of Innovative Computing Information and Control* 7 (2011): 4237-4249.
- [7] C. García-Saura. "Central Pattern Generators for the control of robotic systems." *ArXiv abs/1509.02417* (2015).
- [8] F. Xie, Y. Zhong, R. Du, et al. "Central Pattern Generator (CPG) Control of a Biomimetic Robot Fish for Multimodal Swimming," *J Bionic Eng* 16, 222-234 (2019). <https://doi.org/10.1007/s42235-019-0019-2>.
- [9] Wang, Tianmiao et al. "Learning to swim: a dynamical systems approach to mimicking fish swimming with CPG." *Robotica* 31 (2012): 361 - 369.
- [10] Wang, Shuo et al. "A Bio-Inspired Robot with Undulatory Fins and Its Control Methods." *IEEE/ASME Transactions on Mechatronics* 22 (2017): 206-216.
- [11] C. Zhou and K. H. Low. "Design and Locomotion Control of a Biomimetic Underwater Vehicle with Fin Propulsion." *IEEE/ASME Transactions on Mechatronics*, 17 (2012): 25-35.
- [12] M. Uddin and O. M. Curet. "Modeling and Control of a Bio-Inspired Underwater Vessel with Undulating-Fin Propulsion." *OCEANS 2018 MTS/IEEE Charleston* (2018): 1-7.
- [13] J. Yu, L. Wen, and Z. Ren, "A survey on fabrication, control, and hydrodynamic function of biomimetic robotic fish." *Science China Technological Sciences*, 60 (2017): 1365-1380.
- [14] M. Sfakiotakis, et al. "Experimental investigation and propulsion control for a bio-inspired robotic undulatory fin." *Robotica* 33 (2015): 1062 - 1084.